AN EPFM CRACK GROWTH ANALYSIS OF A 3PB SPECIMEN IN 2D AND 3D

L. G. Lamain

Applied Mechanics Division, CEC, Joint Research Centre, Ispra Establishment, 21020 Ispra (Varese), Italy

ABSTRACT

A FEM crack growth analysis of a 3PB specimen under large scale yielding is presented. Several FE models are used both in 2D and 3D. Crack growth is simulated by releasing the nodes of the crack tip elements (2D) and by shifting the nodal positions at the crack front (3D). The experimental load deflection curve is used as input to the analyses. The obtained J-integral vs displacement curves are compared with the experimental results.

KEYWORDS

FEM; crack growth; 3PB specimen; 3D analysis; J-integral.

1. INTRODUCTION

In the laboratories at JRC-Ispra fracture toughness experiments have been performed on three point bend specimens both for irradiated and unirradiated 316H material and for several temperatures (Bernard, Verzeletti, 1983). In the present paper an extensive FEM analysis is described of one special test piece taken from these experiments.

Several FEM models have been used:
- a 2D mesh with triangular elements focussed at the crack tip, used up to the initiation of crack growth;
- a 2D mesh with quadrilateral elements in the crack plane, suitable to model crack growth by the nodal release method;
- a 3D mesh with one layer of 20-node brick elements over half the thickness;
- a combined 2D/3D mesh with three layers of 20-node brick elements over half the thickness in the crack tip region. The crack growth is obtained by a node shifting procedure.

Performed is a so-called generation phase (Kanninen and co-workers, 1979) or initial filter phase (Shin, De Lorenzi, Andreas, 1979) analysis. For the philosophy behind this type of analysis it is referred to the cited papers.

The experimental load deflection curve is the essential input to these analyses to simulate the experiment and to calculate several fracture parameters. The obtained results serve to interprete the experimental results. Due to several reasons such as discretization of the model, solution procedure of the non-linear equations, uncertainties in the material data, etc., a FEM calculation will furnish only an approximation of the reality. To force the calculation to follow the experimental load line displacement curve it is chosen to modify the uni-axial stress-strain curve slightly, while the non-linear equations are solved as precisely as practically reasonable. Although the main objective of the present analysis is not at all to calculate the stress-strain behaviour, the difference for the 2D and 3D case can be an indication for the validity of the plane strain assumption.

2. EXPERIMENTAL DATA

An unirradiated specimen tested at 550°C was chosen for this analysis. Dimensions of the test specimen are as follows (see Fig.3): length (l) 80 mm, height (w) 20 mm, thickness (b) 15 mm, initial crack length (a) 11.206 mm. The total amount of stable crack growth (Δa_o) is 0.444 mm, this was calculated as a mean of local crack growth in 9 points along the crack front. The crack growth initiation point was established by the potential drop technique and took place at a displacement u = 2.7 mm. The mean crack growth rate $\Delta a/\Delta u$ = 0.126. Young's modulus and Poisson's ratio are according to Aerospace Structural Metals Handbook (1981): E = 1.4 ... $1.6 \cdot 10^5$ MPa (depending on the state of the material), ν = 0.3. The stress-strain curve for this material is given by Matteazzi, Piatti, Boerman (1981) in the form of the Voce relation

$$\sigma = Ae^{C\bar{\varepsilon}_p} + B \qquad (1)$$

At a temperature of 550°C this material shows a strain rate dependency. For a strain rate ranging from $8.33 \cdot 10^{-7}$ to $8.33 \cdot 10^{-4}$, the coefficients of eq.(1) are found in the range A = -926.8 ... -772.2 MPa, B = 1030.4 ... 914.0 MPa and C = -2.633 ... -3.013.

The experimental load line displacement curve is given in Fig.5 and the J-integral vs loadpoint displacement in Figs.6 and 7. This curve is obtained using the formula

$$J = \frac{2U}{b(w - a_o)}$$

where U is the area under the load-point deflection curve.
The dJ/da value for this material shows a normal scatter. An eye fit through 14 data points furnished

$$dJ/da = 1000 \text{ MPa}$$

The analysed specimen was in the lower region of the scatter band, with dJ/da $\sim$ 850 MPa. J_{Ic} = 170 N/mm.

3. ANALYSES

Used for the analyses is the LAMCAL FEM code (Lamain, Blanckenburg, 1982).

This code is based on the displacement formulation and the incremental plasticity theory. All calculations were performed with isotropic hardening and elastic unloading. The tangent modulus solution technique with an original Newton iteration scheme was applied. Convergence criterion is the norm of the out-of-equilibrium forces compared to the norm of the total loading (including reaction forces). The remaining residual load vector was added to the incremental load vector of the next step. Also several modified Newton iteration schemes were tried, in order to reduce the CPU time, but the required tolerance could never be reached for large amounts of plasticity. Nine incremental integration steps of the stress-strain relations are performed every load step and every iteration. In the 2D case three methods to evaluate the J-integral were used: a) Contour integral through nodal points; b) Contour integral through the integration points of the elements, and c) the virtual crack extension method. In 3D only the virtual crack extension method was applied, with a linear interpolation over one element of the local J.

Crack growth was simulated by the nodal release method (2D) and by means of shifting the crack front nodes (3D). In the case of node release first a predictive step was performed to account for the unloading.

3.1 2D Analysis. Both 2D meshes (Figs.1 and 2) consist of 8-node isoparametric elements. Plane strain conditions are assumed.
After scaling to first yield the models were loaded with prescribed displacement steps of Δu = 0.1 mm. Up to three equilibrium iterations were necessary to obtain a norm of the residual load vector almost equal to zero. The load point deflection curve is reproduced very well with both mesh 1 and mesh 2, if the following material data is used: E = $1.5 \cdot 10^5$ MPa, ν = 0.3, A = -916.8 MPa, B = 1031.4 MPa and C = -2.5.

The J-integral vs displacement curve of mesh 1 is somewhat below and that of mesh 2 somewhat above the experimental one. As mesh 1 was designed to serve as a comparison for mesh 2 up to the initiation point, only the results of mesh 2 are reported in this paper (Figs.5 and 6). The crack growth has been modelled by releasing the nodes in the crack plane in the appropriate direction. The reaction forces are put on the new created DOF's in a number of steps with a reversed sign. To obtain a continuous deflection curve, the model was loaded at the same time. Several trials for the crack growth rate and initiation point were made to stay as close to the experimental load line displacement curve as possible. First the experimentally observed crack growth rate of 0.126 and initiation point of u = 2.7 mm were applied. It turn out that in this case the load line displacement curve falls considerably below the experimental one.

Curve 3 in Fig.5 gives an example. Here the initiation point was even taken at u = 3.0 mm and the growth rate was reduced to 0.07. The reaction forces of the released nodes of the crack tip element were decreased in 10 proportional steps. It should be noted that the crack tip element side is only completely released at the 10th step. For simplicity the growth is assumed to be proportional to the decreasing reaction forces. Curve 4 of Fig.5 shows the behaviour of the load deflection curve if initiation is taken at u = 3.6 mm. The crack has been extended by two elements (length of sides each 0.07 mm) with 9 steps of Δu = 0.1 mm for each element. Also this curve falls considerably below the experimental one, especially as compared to the difference between the experimental and the calculated one without crack growth. Curve 5 is the same as curve 4, but the elements are now released in 2 times 14 steps of Δu = 0.1 mm. The experimental curve could be re-

reproduced almost exactly if initiation was taken at u = 4.0 mm with a crack growth rate of 0.05. This curve is not shown on Fig.5 as it coincides with the experimental one. The J-integral curve of Fig.6 is calculated as a mean of several contours, all lying above the experimental one. After crack extension two J-integrals were calculated by virtual crack extension with one and two rings shifted around the tip (curves 4 and 3, respectively, in Fig.6).

3.2 3D Analysis. Mesh 3 (Fig.3) was used with the same material data as for the 2D case. The load point deflection curve falls considerably below the experimental one and no good picture could be obtained from the local J-integral through the thickness. As the CPU time is already rather high (about 2.5 min/step on Amdahl 470/v8), a mesh with more layers over the whole thickness was considered to be not feasible. Therefore, a combined 2D plane strain 8-node/3D 20-node brick mesh (mesh 4, Fig.4) with about the same DOF's as mesh 3 was designed for the final analysis. The 2D and 3D elements are connected by tying the appropriate DOF's. Three layers of 20-node brick elements over half the thickness were used in the crack tip region with thickness ratios of 1:1:1/2 (1/2 at the free surface). At the crack front the elements are collapsed into a wedge shape (extension of mesh 1). Crack growth was modelled by shifting the position of the nodes at the crack front. This was done during a load increment. Due to the high costs only few iterations to follow the deflection curve could be made. With the following data only the first part of the curve could be reproduced,
$E = 1.6 \cdot 10^5$ MPa, = 0.3, A = -877.0 MPa, B = 1000 MPa and C = -2.6.
After scaling to first yield the structure was loaded with prescribed displacement steps of $\Delta u = 0.05$ mm. Three and sometimes four equilibrium iterations were required to obtain a norm of the residual forces of about 10% of the norm of the total forces. Due to the fact that different types of elements were used in the same mesh, the convergence was much slower than in the 2D case.
The global J-integrals were obtained by the virtual crack extension method. The relation between the global J^* and the local J(s) can be written as

$$J^* = \frac{1}{\Delta s} \int_{\Delta s} J(s)\ \delta(s)\ ds$$

where Δs is a portion of the crack front and $\delta(s)$ is the virtual extension, taken linear if J^* is evaluated at a corner node and parabolic if it is evaluated at a midside node.
J(s) can be calculated from J^* if a certain analytical form is assumed. The reported J(s) values in Fig.7 are obtained by assuming a linear variation over one element side. As there are three values J^* available over one element and the value at the midside node is usually much higher than that at the corner nodes (10 - 15%), the linear interpolation is done in a least square sense.
Also other interpolations were performed (e.g. a least square parabolic spline with smoothing) but the reported one was found to be most satisfactory. With all methods the mid-plane values were about the same while the free surface value showed a large scatter (often leading to much lower values than in curve 4 of Fig.7).
The crack growth has been modelled by shifting the nodes of the crack front during a loading step. A constant crack growth rate of 0.126 all along the crack front was applied and initiation was assumed at u = 2.7 mm. These values agree with the experimental ones. The result is graphically given in Fig.7. Other results are given in the following table.

	exp.	mid-plane	calculated mean	free surface
dJ/da (MPa)	850	695	635	200
J_{Ic} (N/mm)	170	225	200	120

4. DISCUSSION AND CONCLUSIONS

The conditions for J controlled stable crack growth can be found at many places in the literature, e.g. Landes (1979):
growth limitations $\Delta a < 0.06\ c$ (c is remaining ligament)

size requirements $w = \frac{c}{J_{Ic}} \left(\frac{dJ}{da}\right) > 10$

$$\rho = \frac{c}{(J/\sigma_o)} > 25$$

$b > c$

For large loads the size requirement for the used specimen is not completely satisfied, so that a violation of the J controlled growth can be expected in that region. This can of course not be the reason why in the 2D case a total stable crack growth of only 0.14 mm could be found. A more plausible explanation is that the plane strain assumptions are only approximately valid. This can also be concluded from the fact that the load line displacement curve of mesh 3 falls considerably below the plane strain one, using the same material data. Furthermore, it seems that node release, applied on relatively large isoparametric 8-node elements, causes such a severe loading condition that the stress and strain state at the crack tip does not represent the reality anymore. This might also be the reason why the J-integral after crack growth shows such a strange behaviour. In fact, during node release, several warnings for a too large load increment were given by the code (unloading and reverse plasticity in one step). These warnings could not be avoided by taking smaller load steps. Node shifting, applied in the 2D/3D case, gives much better results. Conceptually this procedure is also much better than node release as the crack growth rate can be modelled continuously and the structure remains in equilibrium during the extension process. Despite the fact that in 2D/3D the experimental load line displacement curve could not be reproduced exactly in the higher loading range, a total stable crack growth can be predicted that is much higher than in the 2D case. Due to this poor precision and the high costs involved, the calculation was stopped at a displacement of u = 3.7 mm. In the near future the analysis will be repeated with a variable growth over the thickness of the specimen. This will be more in accordance with reality as in the experiment tunneling effects could be noticed. Only the crack tip region was modelled in 3D, but large deformation took place over the whole ligament. A better FE model would be to replace the 2D elements by one layer of 3D elements. The CPU time per step would indeed increase but it is expected that less iterations would be needed to obtain a converged solution. The convergence is very important in this kind of analyses. The change of J-integral in one iteration step can be of the same order of magnitude as the change in J due to the growing crack.

It might also be advantageous to take the thickness of the element at the free surface much smaller than in the present model. In fact, close to the free surface the J-integral drops very rapidly. Curve 4 in Fig.7 gives only a rough indication for the free surface J as the values found with the different interpolations have a very large scatter.

5. REFERENCES

J. Bernard, G. Verzeletti, "Elasto-plastic fracture toughness characteristics of irradiated 316H grade stainless steel", ASTM Symp. Louisville, 20-22 April 1983.

Aerospace Structural Metals Handbook, Vol.2 (1981).

S. Matteazzi, G. Piatti and D. Boerman, "On relating the high-temperature flow stress of AISI 316 stainless steel to strain rate", NETS, Varese, Villa Ponti, 20-22 May, 1981.

J.D. Landes, "Size and geometry effects on elastic-plastic fracture characterization", paper in CSNI report No. 39 (1979), pp.194-225.

M.F. Kanninen et al., "Elastic-plastic fracture mechanics for 2D stable crack growth and instability problems", in Elastic-Plastic Fracture, ASTM STP-668 (1979), pp.121-150.

C.F. Shih, H.G. De Lorenzi and W.R. Andreas, "Studies on crack initiation and stable crack growth", in Elastic-Plastic Fracture, ASTM STP-668 (1979), pp.65-120.

L.G. Lamain, J.F.G. Blanckenburg, "The finite element part of the LAMCAL program - Elastic-plastic fracture mechanics applications", EUR 7999 (1982), Ispra.

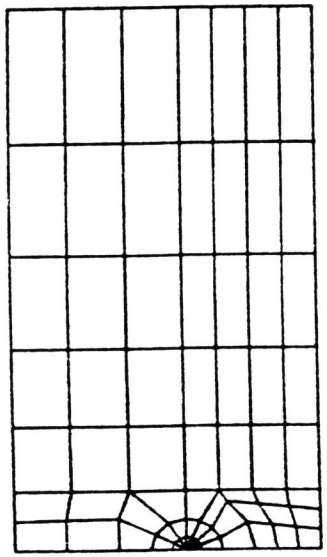

Fig.1 Mesh 1

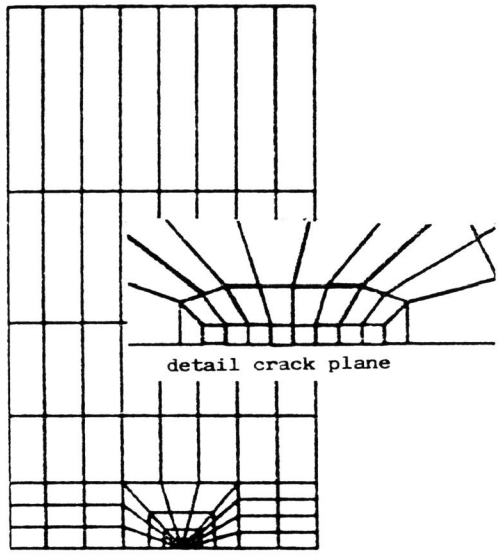

Fig. 2 Mesh 2

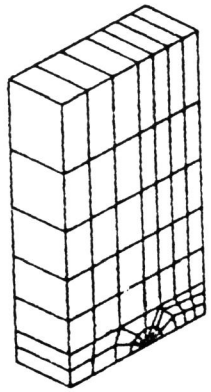

Fig. 3 Mesh 3

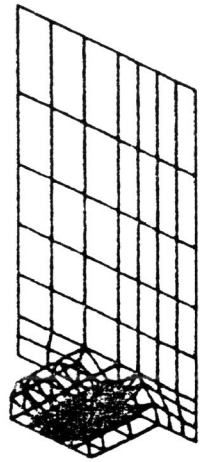

Fig. 4 Mesh 4

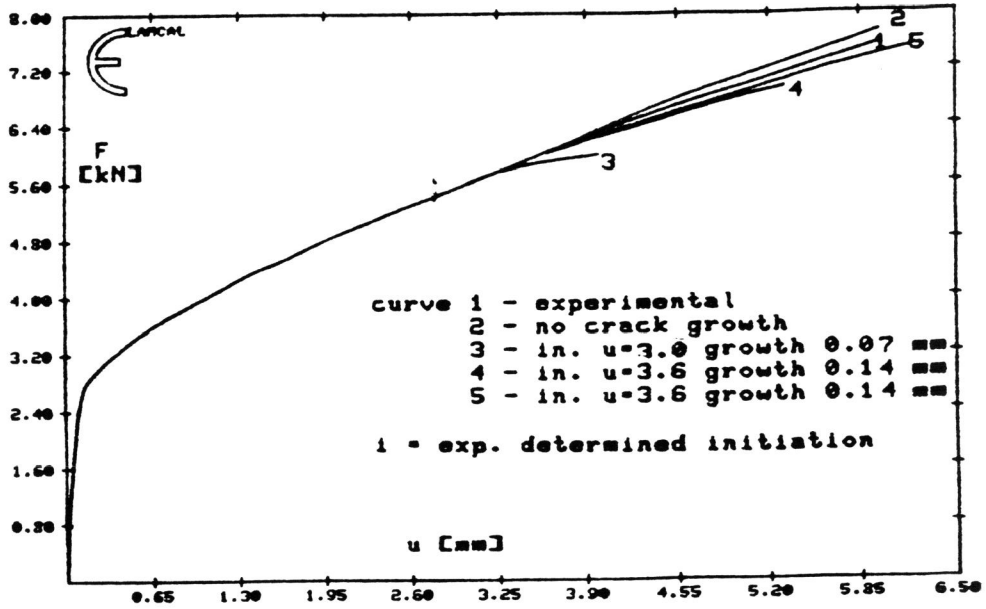

Fig. 5 Load-load point displacement
2D Analysis

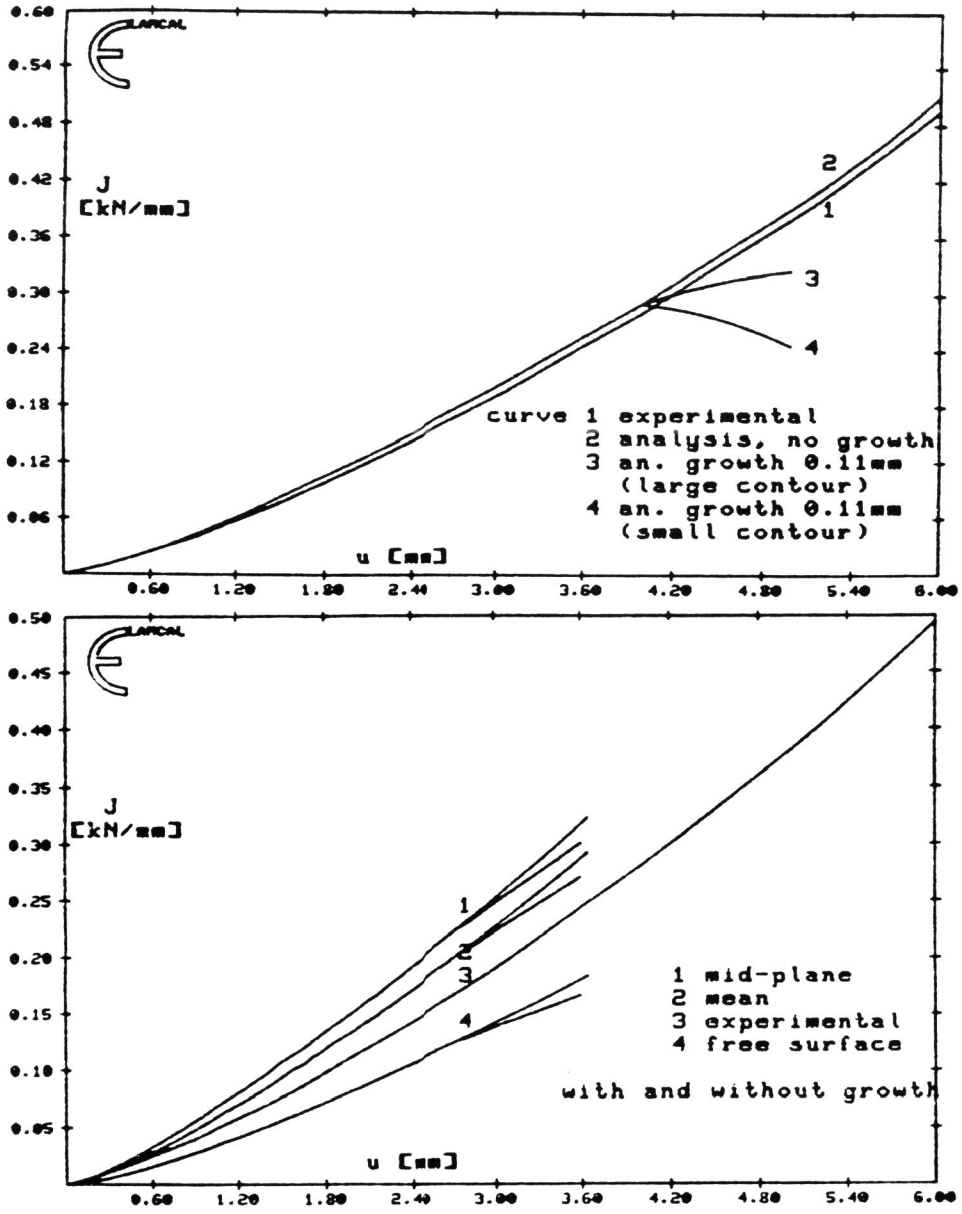

fig. 7 J-integral vs load point displacement
2D/3D analysis